

Structural properties of Cu-Permalloy under annealing

Júlio C. Cezar^{a,b} Marcelo Knobel^b and Hélio C. N. Tolentino^a

^aLNLS CP6192 CEP13084-971 Campinas/SP, Brasil

^bIFGW UNICAMP Campinas, Brasil

E-mail:julio@lnls.br

We have studied the structure of melt-spun copper-permalloy samples ($\text{Cu}_{80}\text{Fe}_4\text{Ni}_{16}$), annealed at several temperatures up to 873 K by means of EXAFS spectroscopy. The results for iron first neighbor average distance showed a slow decrease for annealing temperatures higher than 673 K. The nickel first neighbor distance had almost no change in the whole temperature range. This behavior is discussed in the light of rich iron cluster formation, and is compared with magnetic measurement results.

1. Introduction

Granular alloys composed by a low concentration of magnetic material in a non-magnetic matrix attracted the interest of the magnetism and materials science community because they display giant magnetoresistance effect (GMR) comparable to the one found in multilayered systems (Berkowitz et al., 1992, Yang et al., 1998, Martins & Missel, 1999). Usually the alloy components are immiscible at room temperature, but reach a metastable condition due to a very fast cooling. The concentrations of elements are chosen in such a way that an application of a heat treatment enables the coalescence of the magnetic material, originating magnetic clusters (Allia et al., 1993). The structural properties of these magnetic clusters (e.g., average size, size distribution, concentration) determine the magnetic behavior of the alloy, and its characterization are of key importance to understand the GMR phenomena (Berkowitz et al., 1993).

In this work we performed EXAFS measurements of melt-spun Copper-Permalloy ribbons and from the fitting of these data important structural information were inferred.

2. Experimental details

The samples are melt-spun ribbons of Permalloy diluted in copper, with nominal atomic concentrations $\text{Cu}_{80}\text{Fe}_4\text{Ni}_{16}$. They were annealed in a resistive furnace at 473, 573, 643, 673, 723, 773, 873 K, for two hours. The heating and cooling rates were controlled at 10 K/min.

The measurements were performed at the XAS beam line of LNLS (National Synchrotron Light Laboratory, Campinas, Brazil) (Tolentino et al., 1998). A Si (111) channel-cut monochromator was used to select the energy of the x-ray beam. The spectra were taken at K edge of iron and nickel, in transmission mode, with ionization chambers used as detector of the incident and transmitted beam intensities.

We have measured also the bulk iron, nickel and copper as reference for further data analysis.

3. EXAFS Data analysis

The EXAFS spectra analyzed were the average of at least three individual spectra for each sample at each edge. As the measurements at the iron edges displayed a higher noise level (due to the low iron concentration), in this case some samples were

measured even a higher number of times. Despite this procedure, some spectra at the Fe edge resulted quite noisy. The peaks around 6.2 \AA^{-1} in the samples treated at 673, 723, 773 K comes from a monochromator glitch that were not fully compensated. The resulting $\chi(k)$ signals are showed in figure 1.

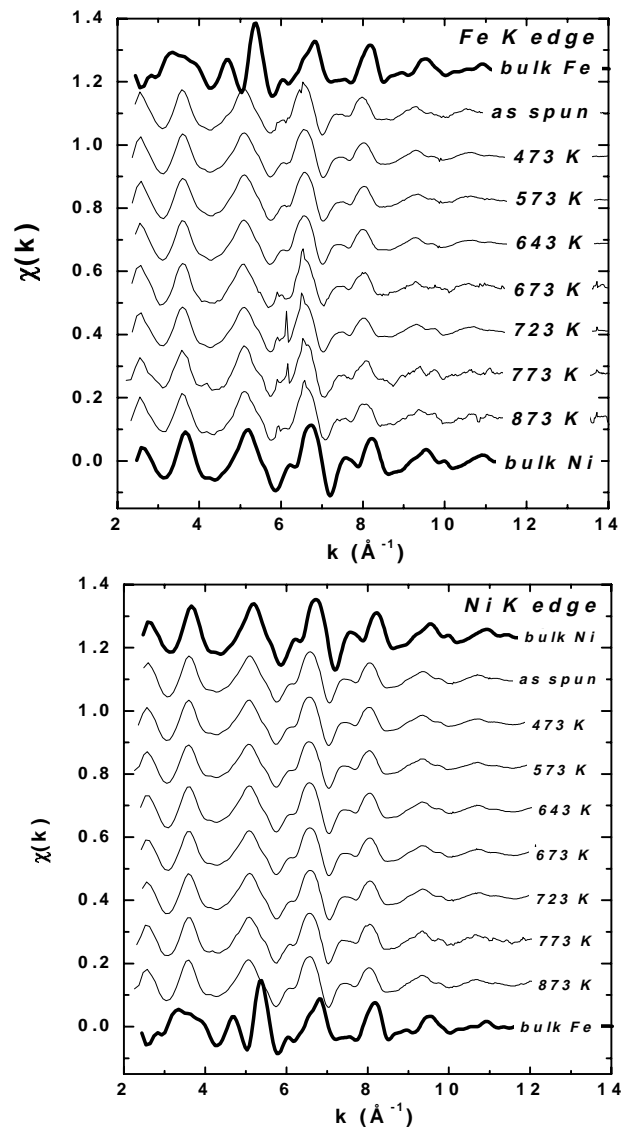


Figure 1

Resulting EXAFS signal, $\chi(k)$, obtained. In the upper panel are shown the spectra at the iron K edge, whereas the results at the nickel K edge are shown in the lower panel. In both panels are included the bulk metals results for comparison.

The following procedure was employed to analyze the data: initially the spectra were averaged. The next steps were performed with the aid of WinXas program (Ressler, 1998). A straight line was fitted to the pre-edge region and subtracted from the whole spectrum. The spectra were normalized at the same point. The edge was then defined as the first root of the second derivative at the edge. The spectra then were changed from energy dependence to photoelectron wave number modulus (k) dependence. The $\chi(k)$ signal were extracted fitting a five-segment spline, weighting the signal by k^2 . The Fourier transforms were performed using a Bessel apodization window, obtaining the pseudo radial distribution

function (p-RDF) for each sample. To isolate the contribution from the first coordination shell, a Fourier back-transform were performed around the first peak of the Fourier transform, resulting in the EXAFS signal correspondent to the first neighbors ($\chi_1(k)$).

Quantitative results were obtained fitting the $\chi_1(k)$ signal. Electronic parameters were obtained from reference metals. To adjust both iron and nickel K edge, we used backscattering amplitude and phases extracted from bulk nickel. This procedure were adopted once that from the p-RDF one can see that iron atoms are also in a local FCC structure, as shown in the next section.

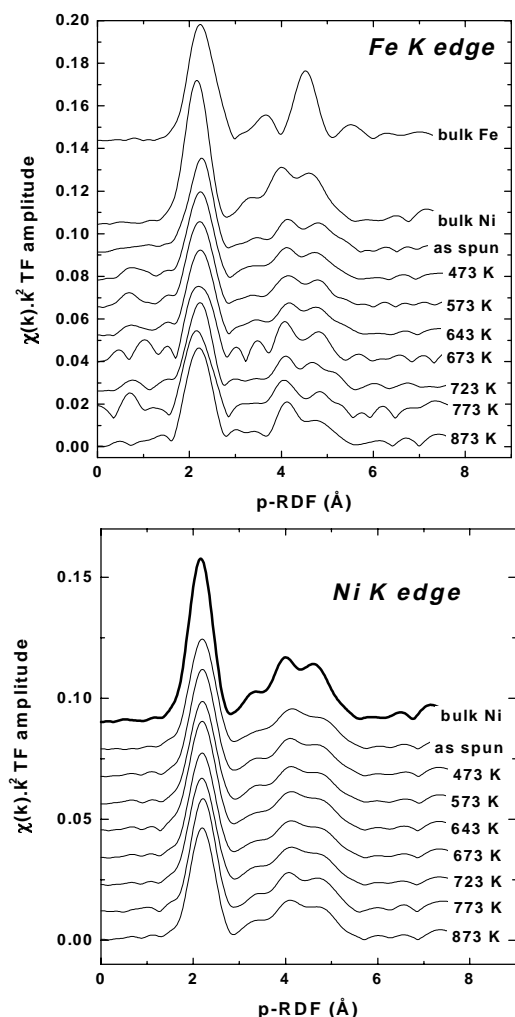


Figure 2

Results of Fourier transform obtained in the data analysis. In the first panel are shown the pseudo-radial distribution functions (p-RDF) for the iron K edge. In this panel is also shown the p-RDF for bulk Ni and Fe. From the comparison among the samples and bulk results, one can see that the iron atoms in the samples have a FCC structure (see text). In the lower panel are shown the resulting p-RDF for the Ni K edge measurements.

4. Results

The annealing of these samples should allow the coalescence of the magnetic materials in the matrix, leading to the cluster formation. This fact is evidenced by magnetization loop measurements that display a faster approach to saturation (of order of 10 J/T.kg) for samples treated at higher temperatures. The magnetization curves of these samples presented superparamagnetic and ferromagnetic components. We calculated the average size of the superparamagnetic clusters, resulting in diameters that range

from 1 nm up to 6 nm (for the as spun and 843 K samples, respectively). These results were published elsewhere (Cezar et al., 2000). Transport measurements on these samples are under way.

To obtain informations about the structure of the magnetic phase in the matrix, initially we looked at the p-RDF obtained from the Fourier transform of the $\chi(k)$ signal. These results are displayed in figure 2. Comparing these results with the bulk reference metals, one can observe that both Ni and Fe atoms carry the FCC signature, for all annealing temperatures. This is expected for a solid solution of $\text{Fe}_{20}\text{Ni}_{80}$ (the nominal Permalloy concentration in our samples). It is worthwhile to note that even the sample treated at 873 K have a FCC structure. Thus, if we assumed that the rich iron cluster are segregated from the matrix, they are small enough to have their structure defined by the matrix. Rich iron cluster are expected once that iron is almost insoluble in copper (Swartzendruber, 1990), whereas the miscibility of nickel and copper is quite high even at room temperatures (Chakrabarti, 1990).

From the fitting procedure of EXAFS data analysis, we have obtained the first neighbor average distance for nickel and iron atoms. These results as function of the annealing temperature are shown in figure 3, where are also indicated the bulk interatomic distances for copper, nickel, FCC iron and $\text{Fe}_{20}\text{Ni}_{80}$ Permalloy. The error bars displayed correspond to a confidence interval of $\sim 69\%$, obtained from the fitting procedure.

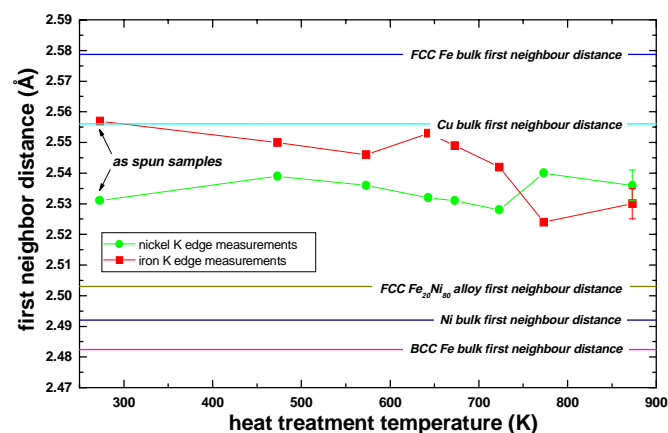


Figure 3

First neighbor average distance results from fitting the first peak in the Fourier transform. The error bars displayed at the 873 K are valid for all data points.

From figure 3 one can see that while the nickel interatomic distance have almost no change with the annealing temperature, the iron interatomic distance presents a decrease for annealing temperatures higher than 673 K. We expect that Ni atoms remain dissolved in the matrix, while Fe atoms are segregated in clusters. This behavior is consistent with our previous observation about the solubility of iron and nickel in copper. Even for the highest annealing temperature, the interatomic distance for iron is higher than that of $\text{Fe}_{20}\text{Ni}_{80}$, which can be result of two situations (or combination of them): i) The true concentration of the cluster is different from the nominal concentration of Permalloy used in the samples. A higher interatomic distance should indicate a higher amount of iron in the particle (an interatomic distance closer to that of FCC iron); ii) The cluster are stressed by the matrix, that has a higher interatomic distance.

In any case, both effects imply in different magnetic properties of the clusters and this information is very important to analyze magnetic measurements in these granular solids. Discussion about the effect on different lattice parameters in FCC iron thin

films can be found, e.g. in Macedo et al., 1998. The dependence of the magnetic properties of Fe-Ni alloys with their concentration can be found, e.g., in Cullity, 1972.

5. Summary and conclusions

We have studied the structural properties of melt-spun and annealed FeNi embedded in a copper matrix. In the whole range of temperatures both iron and nickel atoms presented FCC structure. As the annealing temperature raises, the nickel interatomic distance remained unchanged. On the other hand, for temperatures higher than 673 K, the iron interatomic distance displayed a decrease, but not reaching the distance expected for the Fe₂₀Ni₈₀ alloy. This fact can indicate that the cluster composition is different from the nominal Permalloy composition used in the samples or that the clusters are stretched by the higher lattice parameter of the matrix. In any case, further studies should be performed in this system, once that both situations can affect the magnetic properties of the samples.

Acknowledgements

This work has been partially supported by LNLS. We acknowledge FAPESP for grants and financial support (PROC.N^o 95/06439-4, 98/16329-0).

References

- Allia, P., Tiberto, P., Baricco, M. & Vinai, F. (1993). *Rev. Sci. Instrum.* **64**, 1053-1060.
- Berkowitz, A. E., Mitchell, J. R., Carey, M. J., Young, A. P., Zhang, S., Spada, F. E., Parker, F. T., Hutten, A. & G. Thomas (1992). *Phys. Rev. Lett.* **68**, 3745-3748.
- Berkowitz, A. E., Mitchell, J. R., Carey, M. J., Young, A. P., Rao, D., Starr, A., Zhang, S., Spada, F. E., Parker, F. T., Hutten, A. & G. Thomas (1993). *J. Appl. Phys.* **73**, 5320-5325.
- Cezar, J. C., Knobel, M. & Tolentino, H., in press.
- Chakrabarti, D. J., Laughlin, D. E., Chen, S. W. & Chang, Y. A. (1990). In *Binary Alloy Phase Diagrams*, Massalski, T. B., editor-in-chief, ASM International, Vol. 2, p.1442.
- Cullity, B. D. (1972), *Introduction to Magnetic Materials*, Addison-Wesley, p.526.
- Macedo, W. A. A., Sirotti, F., Panaccione, G., Schatz, A., Keune, W., Rodrigues, W. N. & Rossi, G. (1998). *Phys. Rev. B.* **58**, 11534-11538.
- Martins, C. S. & Missell, F. P. (1999). *J. Magn. Magn. Mater.* **205**, 275-282.
- Ressler, T. (1998). *J. Synchrotron Rad.* **5**, 118-122.
- Swartzendruber, L. J. (1990). In *Binary Alloy Phase Diagrams*, Massalski, T. B., editor-in-chief, ASM International, Vol. 2, p.1408.
- Tolentino, H., Cezar, J. C., Compagnon-Cailhol, V., Tamura, E. & Martins Alves, M. C. (1998). *J. Synchrotron Rad.* **5**, 521-523.
- Yang, Y. K., Chen, L. H., Chang, Y. H. & Yao, Y. D., (1998). *J. Magn. Magn. Mater.* **189**, 195-201.